Journal of Infectious Diseases

DIRECTIVE PUBLICATIONS

ISSN 2831-8064

Research Article

Booster with Intranasal Vaccine Candidate Mambisa Activates the Expression of Tissue Resident Memory T Cell Markers.

Daniel Palenzuela Gardón¹, Diogenes Quintana Vazquez¹, Hamlet Camacho Rodriguez¹, Dania Vazque Blomquist¹, Jorge Aguiar Santiago¹, Heryslina Izquierdo Reinoso¹, Chabeli Rodriguez Ibarra¹, Maité Delgado Espina¹, Anabel Alvarez Acosta¹, Alberto Cintado Benitez¹, Karen Cobas Acosta¹, Iris Valdez Prado¹, Gilda Lemos Pérez¹, Isela María García Tamayo¹, Ingrid Rodriguez Alonso¹, Julio Cesar Aguilar¹, Damian Mainet Gonzalez¹, Amanda Visal Fernandez¹, Rubén Amaya Izquierdo¹, Diosladia Urquiza Noa¹, Pedro Puente Pérez¹, Gerardo Guillen Nieto¹.

Abstract

The study evaluates the efficacy of the nasal booster vaccine candidate Mambisa in the activation of tissue-resident memory T cells (TRM), that are essential in mucosal immunity against respiratory infections such as COVID-19. Mambisa, developed by the Center for Genetic Engineering and Biotechnology (CIGB) in Cuba, combines the RBD protein of SARS-CoV-2 and the HBcAg protein of hepatitis B, and is administered nasally. The preclinical study in mice showed that the nasal administration of Mambisa significantly increased the expression of CD69, and CD103 (TRM markers) in the lungs, while increased FOXP3 expression was also observed. Foxp3 is essential for the development and function of Treg cells, and can influence the activation and regulation of TRM cells. These results suggest that the combination of RBD and HBcAg induces an effective local immune response, with a synergistic effect that enhances TRM cell activation in tissues. Furthermore, mice immunized with Mambisa showed higher RBD-specific IgG antibody titers and increased neutralizing activity against the virus, compared to formulations with only RBD or HBcAg. In a study with nasal samples from 48 COVID-19 convalescent individuals receiving a booster shot with either Mambisa or intramuscular vaccine Abdala significant increases in the expression of genes associated with TRM (CD69, CD103) and effector immune responses (INFG, GZMB, CXCL10) were detected in the Mambisa group, indicating a local activation in the intranasal mucosa. In contrast, there were no significant differences in these markers in the Abdala group. TRM cells, residing in tissues such as the respiratory tract, act as a first line of defense, blocking viral replication and reducing transmission. The Mambisa formulation, by activating these markers, could enhance mucosal immunity, which is crucial in preventing emerging infections and variants. Moreover, the use of HBcAg as an adjuvant improves the RBD antigen presentation, enhancing specific T-cell and antibody responses. In summary, these results suggest that Mambisa is a promising candidate for inducing durable local immunity against SARS-CoV-2, with the potential to reduce transmission and mitigate future outbreaks.

INTRODUCTION

Respiratory infections, such as SARS-CoV-2, begin in the nasopharyngeal tract of the upper respiratory system. It is therefore crucial to establish an immune barrier providing first-line immunity to block infection and transmission. The global vaccination strategy of WHO against COVID-19, has highlighted the importance of mucosal immunity in reducing SARS-CoV-2 transmission, which could prevent the emergence and global surges of new risk variants (1). However, almost all approved COVID-19 vaccines are administered by intramuscular injection. These vaccines induce a systemic

immune response that protects against severe disease and mortality, but are ineffective in generating a mucosal immune response, and do not adequately prevent upper respiratory tract infection and transmission, especially with the emergence of highly transmissible sub-variants.

The factors inducing more effective immune responses via the intranasal route are not fully understood. A suitable approach in this direction could optimize vaccine platforms, in general, and particularly intranasal platforms. The Center for Genetic Engineering and Biotechnology (CIGB) has developed several platforms for the prevention of SARS-CoV-2 infection, which have been shown to strengthen immunity and prevent

*Corresponding Author: Daniel Palenzuela Gardón, Center for Genetic Engineering and Biotechnology, Havana, Cuba, Email: fdaniel.palenzuela@cigb.edu.cu. Received: 27-May-2025, Manuscript No. JOID-4900; Editor Assigned: 28-May-2025; Reviewed: 12-June-2025, QC No. JOID-4900; Published: 26-June-2025, DOI: 10.52338/joid.2025.4900

Citation: Daniel Palenzuela Gardón. Booster with intranasal vaccine candidate Mambisa activates the expression of tissue resident memory T cell markers. Journal of Infectious Diseases. 2025 June; 11(1). doi: 10.52338/joid.2025.4900.

Copyright © 2025 **Daniel Palenzuela Gardón**. This is an open access article distributed under the Creative Commons Attribution License, which permits unrestricted use, distribution, and reproduction in any medium, provided the original work is properly cited.

¹ Center for Genetic Engineering and Biotechnology, Havana, Cuba.

transmission. Abdala, a recombinant protein-based vaccine expressed through the Pichia pastoris yeast, includes the recombinant SARS-CoV-2 receptor-binding domain (RBD) antigen with the aluminum hydroxide gel as its adjuvant. Abdala showed an efficacy of 92.3% (95% CI: 85.7-95.8) in its three-dose intramuscular schedule in the Phase III trial, demonstrating its ability to protect vaccinees (2). Another vaccine candidate in the preclinical phase is Mambisa, one of the five intranasal candidates that have reached clinical trials worldwide (3). Based on recombinant proteins, Mambisa combines the RBD protein of SARS-CoV-2 and the nucleocapsid protein of the hepatitis B virus. Mambisa completed the Phase 2 clinical trial at the National Center of Toxicology (Cenatox, according to its Spanish acronym), demonstrating that it is safe and with preliminary results of its effective immunological action (4).

TRM are a type of T cells that remain in peripheral tissues, both mucosal and epithelial, without recirculating through the bloodstream. They act as a first line of adaptive defense and activate both the innate and adaptive systems. An important marker of the activation of TRMs is CD69, a protein that is overexpressed following immune cell activation that plays a role in the early and late phases of immune responses, thus being crucial for a response against viral infections such as that of COVID-19 (5). This study evaluated TRM activation in lung tissue of mice intranasally immunized with Mambisa and the characterization of TRM activation in the intranasal mucosa of individuals convalescent from COVID-19 for more than 6 months, who received a booster with Abdala and Mambisa. The expression of genes associated with TRM markers such as CD69 and CD103, as well as others related to the defense against SARS-CoV-2 infection, were measured by qPCR.

MATERIALS AND METHODS

Sample collection and total RNA isolation

For the study in mice, 75 Balb/c animals aged 6 to 8 weeks and weighing between 18 and 22g were distributed in 5 study groups. Annex 1 shows the description of the groups, immunogens, volume of administration and number of animals per group. The treatment groups received three sensitization doses. The first 3 administrations were performed every 2 weeks, for pre-sensitizing the animals with the recombinant SARS-CoV-2 RBD protein in the presence of c-di-AMP (CDA). On day 58, groups 1, 2, and 3 received the booster shot, while groups 4 and 5 received it on day 59. The administration was performed via the IN route (50 µl/ mouse) (See Supplementary Figure S1 A). For lung extraction, the thoracic cavity was first dissected and the lungs were removed. The lungs were fragmented into 50-100 mg pieces of tissue and placed in tubes with 1 ml of Allprotect Tissue (Qiagen, Germany). Lung samples in Allprotect Tissue were

incubated overnight at 2-8 oC to ensure a suitable penetration of the reagent. Subsequently, they were stored at -20 oC until their processing to isolate total RNA.

The human study was approved by the CIGB Ethics Committee according to the principles of the Declaration of Helsinki. A written informed consent was obtained from all participants. Forty-eight volunteers that were convalescing from COVID-19 for more than 6 months were randomized into two groups: 26 were treated with one dose of Mambisa in each nostril and 22 with one dose of intramuscular Abdala. Using GDH Gmbh (Germany) swabs, intranasal swab samples were taken from both nostrils before treatment (T0) and 5 days after the treatment (T1) (Supplementary Figure S1 B). Each donor had the swab introduced parallel to the septum up to the inferior turbinate. The swab was then gently rotated on its longitudinal axis from 10 to 20 times. The swabs with the intranasal tissue were introduced in 1 ml of TriReagent and homogenized for 1 min in vortex. Total RNA was isolated using the combined TriReagent/ miRNeasy mini protocol (Qiagen) with on-column enzymatic DNA digestion according to the manufacturer's instructions. Quantification and quality control of the RNA obtained was performed on the Nanodrop 1000 spectrophotometer (ThermoFisher).

Isolation of total RNA

Total RNA was isolated using the combined qiazol/ mirneasy mini (qiagen) protocol with enzymatic DNA digestion in the column, according to the manufacturer's instructions. The CDNA reactions were made using 2 µg of total RNA per sample following the instructions of the First Strand CDNA synthesis kit (cat. No. 04 379 012 001, Roche). The quantification of the RNAs obtained was performed in the Nanodrop 1000 (Themofisher) spectrophotometer. The quality of purified RNA was checked in the Agilent 2100 bioanalyzer. The purified samples were free from genomic DNA, according to the tests performed by QPCR RT +/-.

Reverse transcription

The CDNA reactions were made using 2 μ g of total RNA per sample. In the synthesis of the CDNA anchored- oligo(dT)18 primer AND random hexamer primers were used, according to the procedure of the First Strand CDNA Synthesis Transcriptor Kit (Cat. No. 04 379 012 001, Roche). The reaction was diluted 10 times for a final volume of 400 μ l.

QPCR reactions

QPCR reactions were made using a total volume of 20 μ l. For the mice study, the oligos were used at a concentration of 300 nM, while for the study in humans, the Oligos were used at 500 nM; 10 μ l of LightCyCler® 480 Sybr Green I Master (cat. 04 707 516 001, Roche), 4 μ l of CDNA were added, and the final volume was completed with PCR water quality. The

QPCR runs were made in the LightCyCler 480 II (Roche) team. In the mice study, the genes of interest were CD69, CD103, and FOXP3, while the selected reference genes were MAEA, YWHAZ, RPLP1, HTRP1, and B2M. In the human study with intranasal swab samples, the genes of interest were CD69, CD103, CXCL10, INFG, GZMB, BCL2, TGFB and CASP3. The YWHAZ, RPLP1, HMBS, HTRP1, B2M and UBC genes were used to select the reference genes (Supplementary Table 1).

Immunostimulatory antigens and molecules

The recombinant receptor-binding domain (RBD-H6-PP, residues 331-529) of the spike protein from the SARS-CoV-2 strain Wuhan-Hu-1 (6) was used as the target antigen. The recombinant full-length hepatitis B core antigen (HBcAg) served as the immunostimulatory molecule (7). Both proteins were produced at high purity (≥95%) at the production facilities of the Center for Genetic Engineering and Biotechnology (CIGB) in Havana, Cuba. The c-di-AMP (CDA) was provided with research grade quality by the Helmholtz Centre for Infection Research (HZI) (8). All molecules were tested for lipopolysaccharide (LPS) contamination according to their respective quality systems. For the immunogen preparation, both RBD and HBcAg recombinant proteins were diluted in phosphate-buffered saline (PBS). The lyophilized c-di-AMP (CDA) was dissolved in water before mixing with proteins or, when necessary, further diluted in PBS. To prepare the immunogen, the recombinant proteins were diluted in phosphate-buffered saline (PBS). The lyophilized c-di-AMP (CDA) was first dissolved in water and then mixed with RBD protein. The mixture of RBD and CDA was manually homogenized using a pipette and incubated at room temperature (22°C ± 3°C) for 15 minutes. The immunogen preparations were stored at 5°C ± 3°C until use.

Immunization procedures

The six- to eight-week-old group of 60 female BALB/c mice (H-2d) was sensitized on days 0, 14, and 28 through intranasal immunization with a formulation containing 10 µg of RBD and 5 µg of CDA in phosphate-buffered saline (PBS). A control group of 15 mice was inoculated with PBS. On day 58, the RBD/CDA-sensitized group was randomly redistributed into four subgroups (n=15 each), and the mice were subsequently boosted with one of the following treatments: 1) PBS; 2) Mambisa vaccine candidate (10 μg of RBD and 10 μg of HBcAg per dose); 3) 10 µg of HBcAg per dose; or 4) 10 µg of RBD per dose. The control group only received PBS. To facilitate nasal application, mice were anesthetized with Ketamin. The tip of the pipette was positioned at the surface of each nostril, and the immunogen was gently instilled to allow it to penetrate through the animal's inspiratory airflow. This was done in three cycles of 8.5 µl, 8.5 µl, and 8 µl, for a volume of 50 µl (25 µl per nostril). Blood was collected five days after booster shot and centrifuged to collect serum samples.

Enzyme-Linked ImmunoSorbent assay (ELISA) for antibody measurement

RBD-specific IgG antibodies were assayed as previously described (6). Briefly, 96-well ELISA plates (Corning Costar, Acton, USA)) were coated with 10 µg/mL RBD-H6 antigens overnight at 4 °C, washed with PBST (PBS with 0.05% Tween-20) five times, and blocked with 2% skim milk solution in PBST for 1 h at 37 °C. After washing the plates five times with PBST, serum dilutions or the control monoclonal antibody were added to the plates and incubated at 37 °C for 2 hours. Following a subsequent five washes with PBST, 100 µL of HRP-conjugated antibody (goat anti-mouse IgG, 1:10,000 dilution) was added to the plates and incubated at 37 °C for 1 hour. After five additional washes with PBST under shaking conditions, 100 µL of substrate solution (TMB and hydrogen peroxide) was added to each well. Upon completion of a 10-minute reaction, 50 µL of stopping solution was added to each well. Absorbance was measured at 450 nm using a microplate reader (BMG Labtech, Ortenberg, Germany). Serum IgG antibody titers were expressed in arbitrary units (AU) relative to the SARS-CoV-2 monoclonal antibody AcM02 (CIGB SS).

Plate-based RBD to ACE2 binding assay

The inhibitory activity of anti-RBD polyclonal sera on the binding of an RBD-HRP conjugate to hFc-ACE2-coated plates was assessed as previously described (7). ELISA plates (Costar 3591) were coated with 0.25 µg per well of recombinant hFc-ACE2 in PBS for three hours at 37°C, followed by washing with 0.1% (v/v) Tween-20 in distilled water and blocking with 2% (w/v) nonfat dry milk in PBS for one hour at 37°C. Mixtures of the RBD-HRP conjugate (CIGB, Cuba; diluted 1:100,000) and serial dilutions of sera in 0.2% (w/v) skim milk in PBS were preincubated for one hour at 37°C, with a monoclonal antibody, CBSSRBD-S.8 (CIGBSS, Cuba), serving as a positive control due to its strong neutralization activity against SARS-CoV-2. After four washes with 0.1% (v/v) Tween-20 in distilled water, the sera-conjugate mixtures were added to the hFc-ACE2-coated wells and incubated for another hour at 37°C. A substrate solution containing TMB and hydrogen peroxide was then added, and after a 10-minute incubation at room temperature, the reaction was stopped with the 2M HOSO solution. The optical density of the microtiter plates was measured at a wavelength of 450 nm. Inhibition values were calculated using the formula: Inhibition (%) = (1 - sample optical density value/negative control optical density value) × 100, with results expressed as percentages and a positivity threshold set at 20%. Data were plotted using GraphPad Prism version 8.0.2, and the surrogate neutralization titer was defined as the concentration yielding 50% inhibition (IC50), determined using the log of the inhibition value vs. normalized response variable slope model.

Statistical processing

Statistical analyses were performed using Genex software (MultiD AB, Sweden). Statistical preprocessing of the data followed the recommendations described by Bergkvist et al. (9). Additionally, the multivariate statistical R libraries included Factominer, FactoExtra, and FactoInvestigate in order to conduct principal component analysis (PCA). The algorithms used in the selection analysis for the best reference genes were NormFinder (10), GeNorm (11), and RefFinder (12), which also integrate data from BestKeeper (13), and DeltaCt (14).

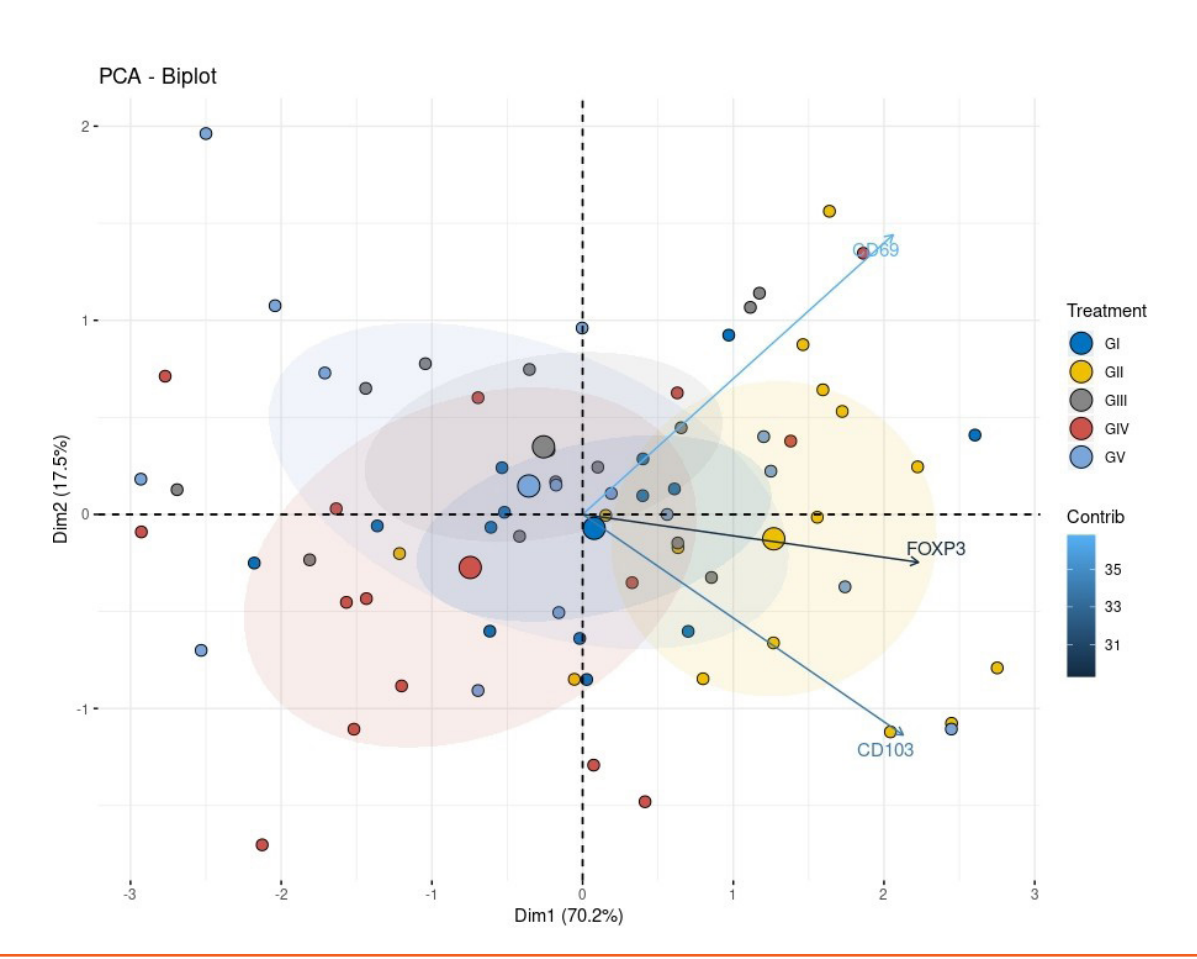
RESULTS

Mambisa activates the expression of TRM markers in mouse lung tissue

From the reference gene study in mice, the most stable gene was GUSB, and the GUSB/HPRT1 pair was selected, within the consensus variant, as the best gene combination among the different algorithms. PCA tool provides an overview of the complexity and interrelationships of multivariate data sets. It is able to reveal relationships between variables and between samples (e.g. patterns), detect outliers, find and quantify patterns and trends, and extract and compress multivariate data sets, among other applications (15,16). One of the premises of the PCA is that there is a correlation between the variables in the data matrix. Pearson's correlation matrix showed that there are significant correlations between the variables. In addition, Bartlett's test of sphericity shows a significant correlation in the data indicating the possible use of a PC (Chisq(3) = 63.62, p << .001). Additionally, the Kaiser, Meyer, Olkin overall measure of sampling adequacy (KMO) suggests that the data are appropriate for performing the PCA test (KMO >= 0.65).

The PCA biplot shows the scores of the observations (samples) as points, and the loadings of the variables as vectors in a two-dimensional space, representing the multidimensional relationships of the data. This type of analysis helps visualize the relationships between the samples and variables (17,18). The biplot graph (**Figure 1**) shows that the first and second dimensions explain 70.2% and 17.5% of the variability of the data, respectively, for 87.7% of the total inertia of the data set. The graph shows that all three vectors are directed towards the Mambisa group cluster (GII), indicating that samples in the Mambisa group tend to have an increased expression in the three genes studied, compared to the rest of the groups. All three vectors have a significant correlation with the first component. FOXP3 shows the highest contribution followed by CD69 and CD103 (Supplementary Table S2). These results support the fact that Mambisa activates the expression of these genes.

Figure 1

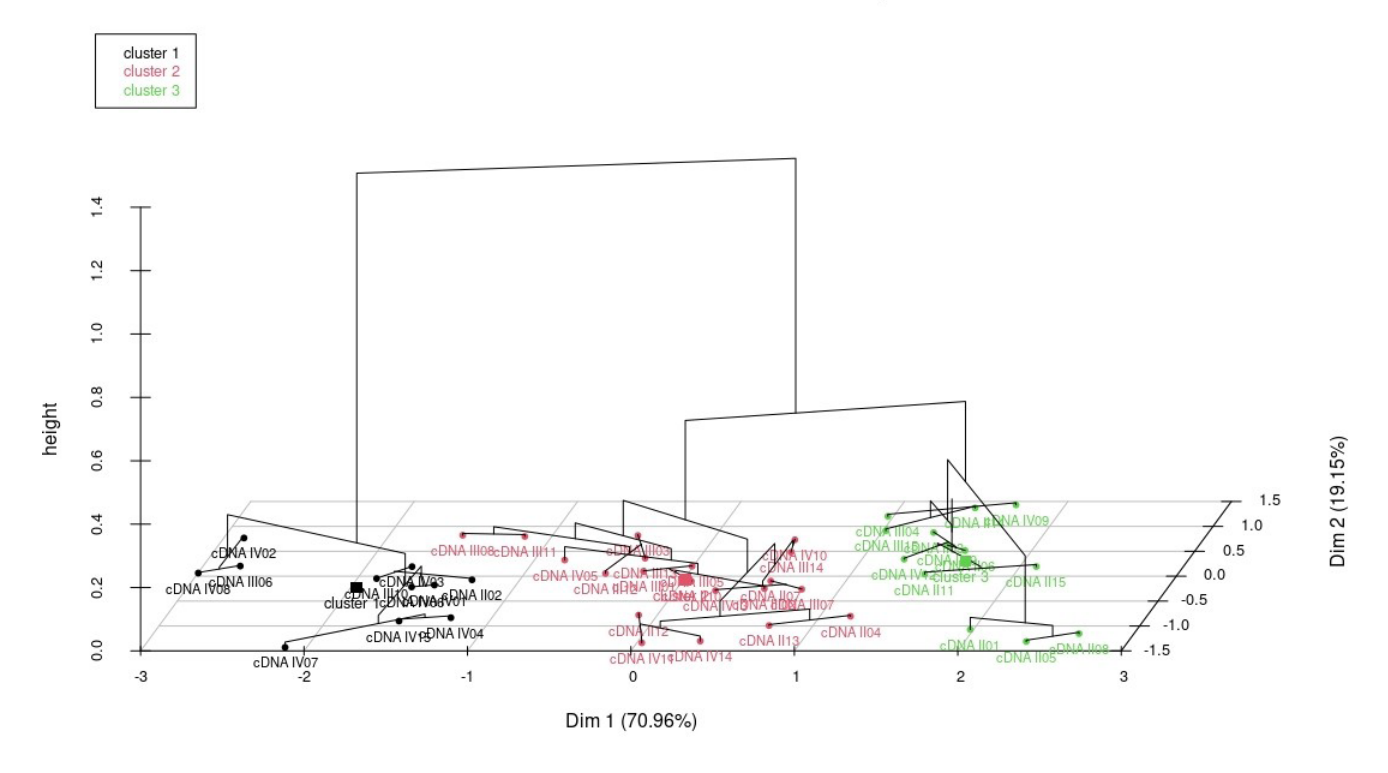


Biplots of the principal component analysis performed on the interaction between variables (genes) and treatments. GI-PBS/sensitized, GII-Mambisa, GIII-HBcAg, GIV-RBD, and GV-PBS.

The analysis of the centers of inertia infer that the Mambisa, HBCAg and RBD treated groups can be segregated in clusters, with different expression patterns. This was confirmed in the unsupervised hierarchical cluster analysis with data from the three groups. Hence, the samples were grouped into three separate clusters (**Figure 2**). Cluster 1 mainly grouped the GIV samples, cluster 2 contains the GIII samples and cluster 3 contains the GII samples. This result supports the hypothesis that the activation effect of the genes studied in the Mambisa group is due to a synergistic interaction between HBcAg and RBD compounds.

Figure 2

Hierarchical tree on the factor map



Ascending hierarchical cluster analysis for groups GII(Mambisa), GIII(HBCAg) and GIV(RBD). GIV samples were mainly grouped in cluster 1, GIII samples were grouped in cluster 2 and GII samples were grouped in cluster 3.

The means of the groups were compared using parametric statistics. According to the Kolmogorov-Smirnov test, all groups compared fit the normal distribution, so the t-test with the p-value correction was used for multiple comparisons. The post hoc power analysis showed that according to the number of samples and the experimental variability, differences of 0.45 are detected with a power of 80%. Annex 2 shows the results of the mean comparisons between the groups for each gene. The group treated with Mambisa (GII) has the highest expression of the three genes; this difference was significant compared to the means of the GI, GIII and GIV groups. Statistically significant differences were only observed for the CD69 gene when the means of GII (Mambisa) and GIII (HBCAg) were compared.

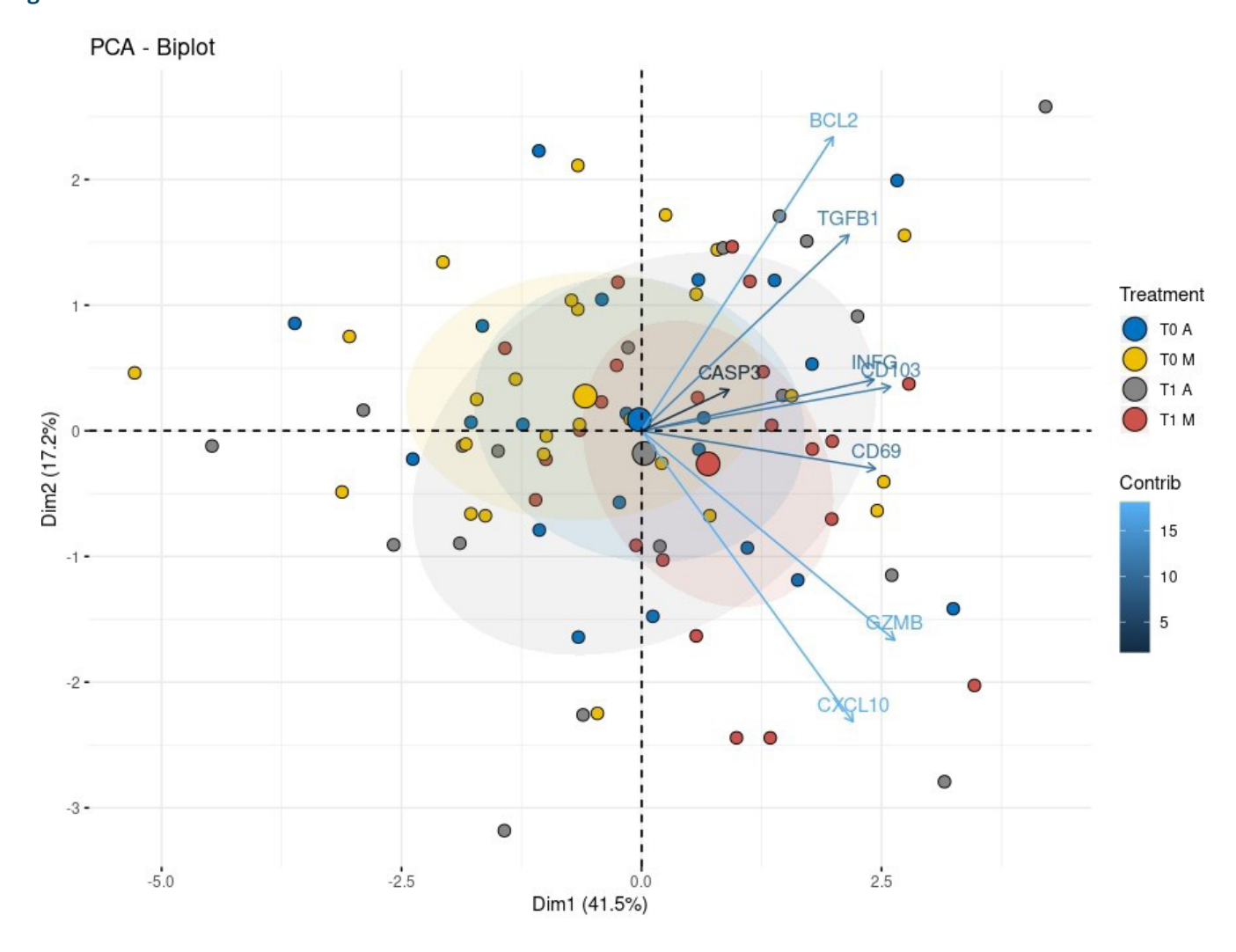
Mambisa activates the expression of TRM markers in the mucosal tissue of post-COVID-19 individuals

The study of reference genes in the mucosal tissue of post-COVID-19 individuals showed that the most stable gene was YWHAZ and the pair YWHAZ and B2M was selected among the best gene combinations because it showed the best reduction of variability observed in each gene after normalization. Correlation analyses showed that there were significant correlations between the variables. In general, correlation clusters are observed; Bartlett's test of sphericity suggests that there is sufficient correlation in the data to perform PCA (Chisq(28) = 253.56, p < .001). Additionally, the Kaiser, Meyer, Olkin test (KMO), an overall measure of sampling adequacy, suggests that the data are suitable for the PCA (KMO = 0.63).

The PCA yielded that the first two dimensions explain 58.76% of the total inertia of the data set; this value is much higher than the baseline value of 37.2%, therefore, the variability explained by this plane is significant. **Figure 3** shows the biplot analysis

where we find that the centers of inertia for the Abdala-treated group are close together and near the center of the plane, indicating that there is no differentiation in the expression pattern between time T0 and T1 for the Abdala group. However, in the Mambisa group the centers of inertia for times T0 and T1 are separated in the second and fourth quadrants, respectively. The p-value of Wilks' test indicates that the categorical variable (Treatment group) explains the separation between individuals, where the Mambisa T1 category is significant in this case (p-value = 0.03).

Figure 3



Biplot of the principal component analysis performed on the interaction between the variables (genes) and the Abdala and Mambisa treatments.

The most important genes explaining the variation observed in dimension 1 are GZMB, CD103, CD69, and INFG, while in dimension 2 those are the genes BCL2, CXCL10, GZMB, and TGFB. Notably, in dimension 3 the highest contributing gene is CASP3. In general, as a trend, all vectors (genes) move in the direction of the Mambisa treated group, showing an increase in gene expression in this group. In particular, an increase in the expression of genes related to resident T memory CD69 and CD103 is observed.

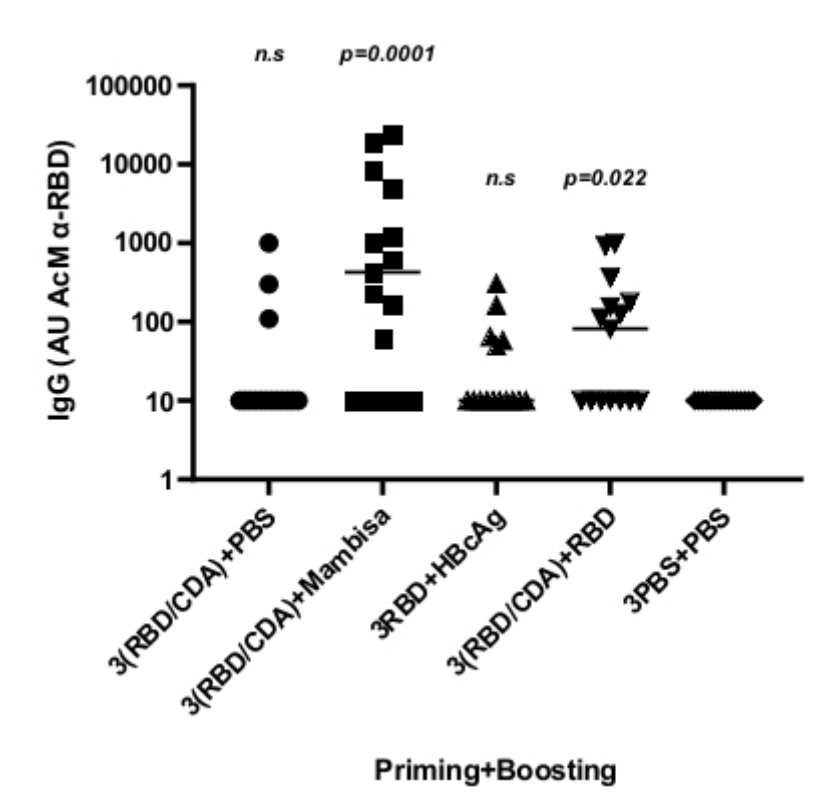
In the parametric statistical analysis, the Kolmogorov-Smirnov test showed that not all groups complied with the normality condition, so the Wilconxon test was used for the paired analysis. According to the results of this test, significant statistical differences were found only in the Mambisa treatment, particularly with the INFG, CD69, GZMB, and CXCL10 genes. The CASP3 gene presented a p-value near the statistical significance limit of 0.05. For the Abdala treatment, no significant differences were observed.

Characterization of the humoral response in mouse

During the study, there was no weight loss or symptoms of respiratory inflammation in the mice, nor were there signs of damage upon lung extraction. The RBD/CDA-intranasally (i.n) sensitized mice were further boosted with the following treatments: 1)

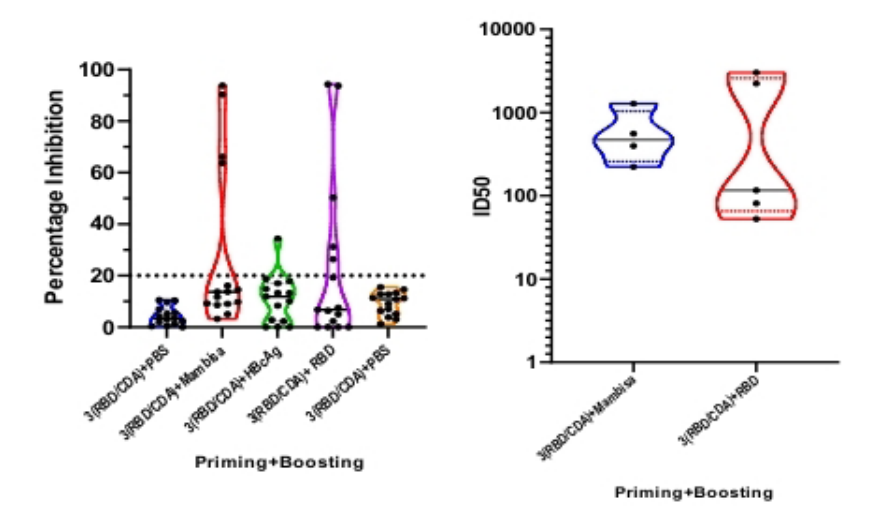
PBS, as the antigen-free control; 2) RBD+HBcAg, the Mambisa candidate vaccine; 3) HBcAg, as the immunomodulatory antigen control; 4) RBD, as the target antigen control. The non-sensitized mice (negative control) treated with PBS were further treated with PBS. Compared to the negative control, the i.n. booster immunization with Mambisa (RBD+HBcAg) induced a significant early RBD-specific IgG response (p < 0.001) (**Figure 4**). There was a significant increase in antigen-specific IgG with sera samples from mice boosted with the RBD (p < 0.02). In contrast, no significant RBD-specific IgG response was found in sera samples from mice boosted with HBcAg or PBS (p > 0.05). The sera from mice boosted with Mambisa and RBD treatments with the positive inhibition activity of ACE2-RBD binding presented IC50 of 780AU and 180AU respectively (**Figure 5**). The only low titers (< 50 AU) and frequency of response (2/15) for IgG or IgA antibodies were detected in the intranasal washes of mice boosted with Mambisa alone (data not shown). In mice boosted with Mambisa and RBD, a positive and significant linear relationship was observed between IgG antibody titers and percentage of inhibition (Figure 6). Only the mice boosted with Mambisa showed sample sera with positive binding activity (≥20%) characterized by relatively high IgG titers (≥5000AU) and high inhibitory activity (≥60%).

Figure 4



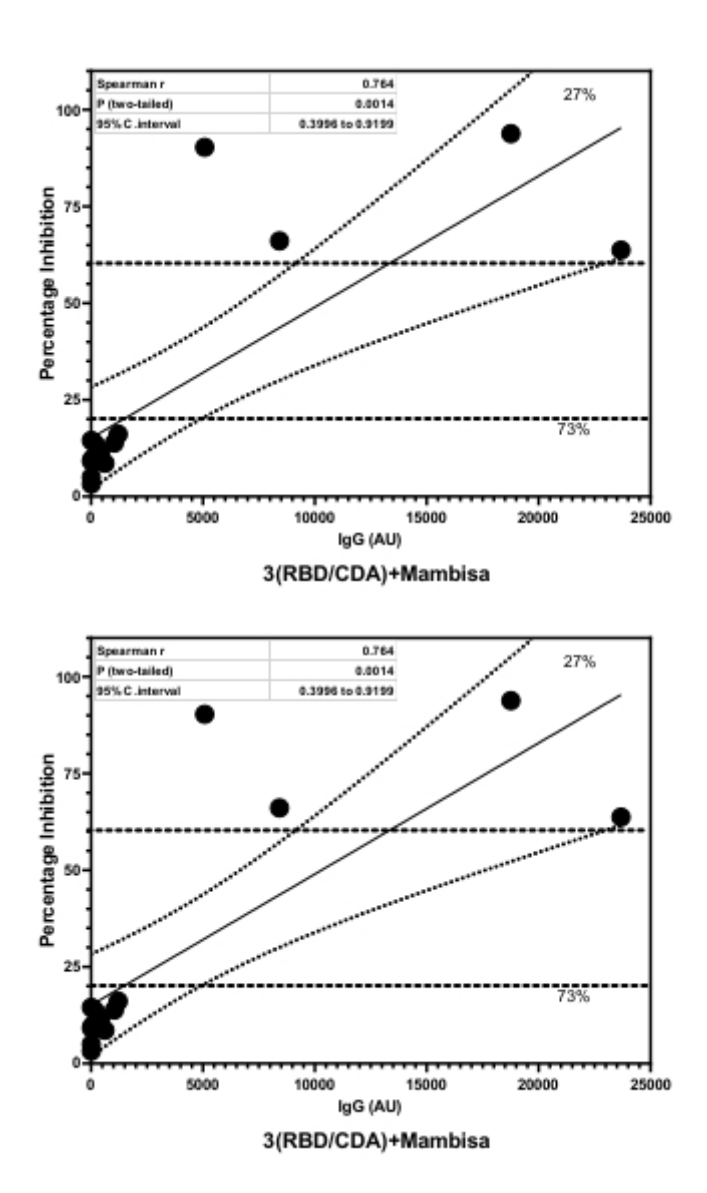
Early effect on serum IgG production against RBD after boosting with Mambisa in mice primed with three RBD/CDA shots. Levels of specific IgG against RBD were assessed by ELISA five days after boosting, using sera from mice of the five experimental groups. Statistical significance for the comparison with the negative control group treated with PBS throughout the vaccination schedule was assessed by the Kruskal-Wallis ANOVA test, followed by Dunn's multiple comparisons test. Significant differences are indicated by the probability value in each graph. n.s. = not significant.

Figure 5



Activity of polyclonal sera to inhibit the binding of RBD to the ACE2 receptor. A highly neutralizing monoclonal antibody was used as the positive control. The dashed line represents the effective activity threshold (≥20%). Positive samples were characterized by their surrogate neutralization titer, defined as the concentration yielding 50% inhibition (IC50).

Figure 6



Linear relationship between IgG antibody titers and inhibitory activity of polyclonal anti-RBD sera. Dashed lines establish three arbitrary levels of inhibitory activity: negative (<20%), moderate (20%-60%) and high (>60%). Percentage values indicate the proportion of sera with inhibitory activity at each level.

DISCUSSION

The activation TRM is a critical element in the regulation of immune responses, particularly in relation to local immunity and the preservation of immune homeostasis. These cells, which inhabit non-lymphoid tissues, are essential in providing rapid immune defense in the case of subsequent exposure to pathogens and in dealing with tissue-specific challenges. Accordingly, the activation of TRM by SARS-CoV-2 vaccines represents a crucial aspect of the immune response, especially in regard to effective vaccine strategies aimed at fighting viral pathogens. The ramifications of its activation by SARS-CoV-2 vaccines are complex and encompass the enhancement of local immunity, long-lasting protection, and the ability to mitigate the impact of emerging viral variants.

TRM cells are distinguished by unique surface markers, including CD69, CD103 and CD49a, which facilitate their retention in tissues and define their functional capabilities. The activation of these specific markers is essential for the conservation and effector functions of TRM cells. For example, CD69 is involved in the inhibition of sphingosine-1-phosphate receptor 1 (S1P1), which favors the retention of T cells in tissues by obstructing their outflow into lymphatic vessels. This retention is essential during the initial stages of an immune response, as TRM cells are able to initiate rapid responses to reinfection at the entry site of the pathogen, often leading to more rapid resolution of infections compared to circulating memory T cells (19).

Moreover, CD103 expression identifies a set of TRM cells that are particularly effective in responding to epithelial infections. A recent report demonstrated that CD103+ TRM cells have superior cytotoxic functions and can rapidly secrete effector cytokines, such as interferon gamma (IFN-gamma) and tumor necrosis factor-alpha (TNF- α), upon re-exposure to antigens (20). These cytokines are critical in orchestrating localized immune responses, stressing the importance of TRM cell activation markers in their immediate protective actions against pathogens.

The function of TRM cells goes beyond the provision of immediate immune responses, they also play a crucial role in promoting long-term immunity against various pathogens. For example, CD8+T cells residing in airway tissues have been shown to obstruct the transmission of respiratory viruses, including heterosubtypic strains of influenza, through their ability to proliferate rapidly and produce high levels of IFN during secondary infections (21).

The activation of T resident memory (TRM) cells has a significant impact on cancer immunology. Molodtsov et al. demonstrated that the infiltration of tumors with TRM cells correlates with improved patient prognosis, indicating their pivotal role in antitumor immunity (22). The identification of markers of TRM cell activation in tumor microenvironments can provide critical information on therapeutic methods for enhancing the functionality of these immune entities. For example, the expression of CD103 and CD69 cells on tumor-infiltrating lymphocytes is associated with favorable clinical outcomes in various malignancies, suggesting that strategies designed to promote TRM activation could amplify antitumor immune responses (23).

A major advantage of TRM cells lies in their ability to elicit immediate immune responses at pathogen invasion sites. The localization of these cells in tissues, such as that of the pulmonary system, is particularly vital for the control of respiratory viruses, including SARS-CoV-2. Therefore, immunization strategies that enhance the recruitment and activation of TRM cells can significantly boost local immune defense, which could mitigate viral load and transmission dynamics (20).

The generation of TRM cells is closely related to the establishment of a long-lasting immunological memory, which is crucial for sustained protection against subsequent infections. Research shows that these cells can remain in various tissues long after initial antigen exposure, and act as reservoirs for immune defense. This persistence is especially important in the context of SARS-CoV-2, given the observed decrease in humoral immunity following vaccination (24,25). Activation of TRM cells may also play a key role in the crossreactivity of the immune response against new variants of SARS-CoV-2. Reports indicate that memory T cells elicited by vaccination can recognize conserved viral epitopes, thus maintaining their efficacy against the mutated strains (26). This cross-reactivity highlights the need to target multiple viral antigens during vaccine development to elicit broad and potent T-cell responses (27). While antibody-mediated responses are crucial in obstructing initial infections, the contribution of TRM cells to a comprehensive immune response is critical. Their activation serves to complement the humoral response by providing localized protection and facilitate the elimination of infected cells (28).

In mice, intranasally immunized with HBcAg/RBD and CDA, we showed that this combination could enhance the stimulation of TRM identification markers, and also innate immunity (paper in press). In the current study we demonstrated that the intranasal administration of Mambisa activates TRM response at the level of the intranasal mucosa in post-COVID individuals. In the PCA a trend observed is that all vectors (genes) move in the direction of the Mambisa treated group (Figure 3), evidencing an increase in gene expression. This

increase in the expression of genes related to the TRM response such as CD69 and CD103 was also observed in other markers, such as GZMB, INFG, CXCL10, and TGFB that are important in the immune response against viral infections (29–31). Furthermore, we observed TRM activation in lung tissue in mice (Figure 1). Its importance lies in that the respiratory viruses are located and reproduce in this organ, producing serious health conditions. We also found that the molecular action of the Mambisa vaccine candidate activating the TRM response in the lung tissue may be due to a synergistic effect between HBcAg and the RBD fragment. Hierarchical cluster analysis (Figure 2) suggests this effect, given the difference in the expression profile. Our results can support the efficacy of the Mambisa intranasal candidate in combating respiratory infections such as SARS-CoV-2 since the presence and functional capacity of TRM cells are correlated with protective immunity (32). Moreover, we observed an increased expression of FOXP3 in the Mambisa group. The Foxp3 gene plays a key role in the activation and function of regulatory T cells (Treg), which are essential for maintaining immune tolerance and preventing autoimmunity. Foxp3 is also essential for the development and function of Treg cells, which in turn influence the activation and regulation of TRM cells. In tissues, Foxp3+ Treg cells regulate the local immune environment and suppress excessive immune responses and maintain tissue. They therefore, maintain tissue homeostasis and prevent autoinmunity. This regulatory function is critical in preventing immunopathology during infections and autoimmune diseases (33,34). FOXP3-expressing Tregs are essential in maintaining immune homeostasis and preventing autoimmunity. Recent studies highlight their role in modulating TRM responses. For example, type 1 Treg, expressing both Foxp3 and transcription factor T-bet, promotes CD8+ TRM generation by regulating the bioavailability of transforming growth factor β (TGF- β) in the tissue microenvironment (35) . This mechanism ensures that TRMs are properly established and functional. The development of TRM is influenced by Foxp3+ Treg cells, which facilitate the expression of CD103 on CD8+ T cells, a marker of tissue residence (36). In the absence of Treg cells, the generation of memory CD8+ T cells is impaired, thus reducing the formation and function of memory CD8+ T cells (37). This emphasizes the importance of Foxp3 in the evolutionary trajectory of TRMs. According to our results, Mambisa can potentiate the interaction between Foxp3+ Treg cells and TRM cells.

The receptor-binding domain (RBD) located in the spike protein of SARS-CoV-2 is an effective protective determinant against the virus and is included in a commercial and highly effective vaccine (38,39). In the present study, three doses of the RBD+CDA immunogen were administered to naive mice to establish pre-existing specific immunity to RBD. Pre-sensitized groups of mice with the RBD+CDA immunogen received a

booster dose with the above described immunogens. The sera collected on day 5 post-boosting (the same day the lungs were harvested to evaluate genetic markers associated with resident memory) were assessed to determine the ability of these immunogens to activate the IgG antibody response against RBD. The Mambisa immunogen (RBD+HBcAg) induced higher IgG antibody titers with greater inhibitory activity.

The HBcAg protein was previously cidentified by Aguilar et al as a potent immune modulator that enhanced both humoral and cellular specific responses to vaccine antigens (40). The observed enhancement is attributed to the unusual dimeric alpha-helical structure of the HBcAg protein, allowing it to assemble into high density particles of protruding spikes. This unique feature of HBcAg plays a crucial role in improving its functional activity as an adjuvant to induce an enhanced immunological response (41). Notably, Aguilar et al. conducted their study in naïve mice, administering intranasal formulations of mixed HBsAg and HBcAg antigens via a homologous prime-boost regimen, with evaluation performed 10 days after the final dose.

However, in the present study the Mambisa immunogen (RBD+HBcAg) was administered in a heterologous primeboost regimen. Therefore, the qualitative differences observed relatively earlier (Day 5), which enhanced the response generated after boosting with Mambisa, may also be explained by the establishment of a functional optimized ratio between CD4+ helper T cells and CD4+ FoxP3+ regulatory T cells specific to the RBD protein. The Mambisa immunogen may have promoted relatively lower counts of RBD-specific CD4+ FoxP3+ T cells or is functionally less effective than other formulations, thereby predominantly favoring the expansion and productivity of anti-RBD effectors. It is noteworthy that this observation corresponds to a short time frame after boosting, hence the observed effects were still under development. New studies are therefore needed to clarify these features. Although these immunological factors were not evaluated in our study, this regulatory T cell-mediated model has been associated with increased vaccine efficacy and reduced lung injury (42).

Our study demonstrates that the Mambisa intranasal vaccine candidate enhances the expression of TRM, which are critical components of the immune response and key to both immediate and sustained protection against viral infections such as SARS-Co-2. Additionally, we observed an early increase in serum IgG antibodies targeting the receptor-binding domain (RBD) in mice that received a Mambisa booster shot following three RBD/CDA vaccinations. These findings highlight the importance of further investigating the mechanisms underlying memory T-cell responses induced by vaccine candidates. Such insights will be essential to guide the design of next-generation vaccines and sustained public health strategies to combat the virus in the current

epidemiological 'new normal' scenario, thereby preventing future respiratory virus outbreaks.

Acknowledgement

We thank Mirian Rivas Hermelo for critical reading of the manuscript.

Data availability statement

The raw data supporting the conclusions of this article will be made available by the authors, without undue reservation.

Ethics statement

Ethical approval for the human and animal studies were approved by the CIGB Ethics Committee according to the principles of the Declaration of Helsinki. The studies were conducted in accordance with the local legislation and institutional requirements.

Author contributions

DPG, and DQV designed experiments, analyzed data, writing-original draft, writing-review and editing.

JAS and GGN designed experiments.

HCR, DVB, HIR, ACB, and DMG conducted the gene expression experiments.

CRI, MDE, AAA, KCA, IVP, and IMGT processed human and mouse samples.

GLP conducted detection and quantification of cytokines.

RAI, DUN, and PPP conducted mouse experiment.

Funding

The author(s) declare that financial support was received for the research, authorship, and/or publication of this article. This work was supported by the National Science, Technology and Innovation Programs of Cuban Ministry of Science and technology.

Conflict of interest

The authors declare that the research was conducted in the absence of any commercial or financial relationships that could be construed as a potential conflict of interest.

Supplementary Table S1. Sequences of synthetized gene primers.

Mouse study					
Gene	Sequence (5'->3')	Template strand	Length		
CD69	Forward primer	GGAGAGAGGCAGAAGGACCAT	22		
	Reverse primer	AGGTAGCAACATGGTGGTCAGA	22		
CD103	Forward primer	CCAGAGTCAAGAGCCTGCGT	20		
	Reverse primer	TCACCAAGGATCGGCAGTTCA	22		
FOXP3	Forward primer	ATGGCAATAGTTCCTTCCCAGA	22		
	Reverse primer	ATTGAGTGTCCTCTGCCTCTCC	22		
B2M	Forward primer	ACC GTC TAC TGG GAT CGA GAC A	22		
	Reverse primer	TGC TAT TTC TTT CTG CGT GCA T	22		
RPL13a	Forward primer	ACA AGA AAA AGC GGA TGG TGG T	20		
	Reverse primer	TTT CCT TCC GTT TCT CCT CCA G	20		
HPRT1	Forward primer	TCAGTCAACGGGGGACATAAA	21		
	Reverse primer	GGGGCTGTACTGCTTAACCAG	21		
MAEA	Forward primer	TGATGGTGGAGCATCTGCTACG	20		
	Reverse primer	CCTCCACTTCTTTGGCTGTCAG	21		
YWHAZ	Forward primer	AACAGCTTTCGATGAAGCCAT	20		
	Reverse primer	TGGGTATCCGATGTCCACAAT	20		
		Human study			
Gene	Sequence (5'->3')	Template strand	Length		
ACTB	Forward primer	CTGGAACGGTGAAGGTGACA	20		
	Reverse primer	AAGGGACTTCCTGTAACAATGCA	23		
B2M	Forward primer	TGCTGTCTCCATGTTTGATGTATCT	25		
	Reverse primer	TCTCTGCTCCCCACCTCTAAGT	22		
HMBS	Forward primer	GGCAATGCGGCTGCAA	16		
	Reverse primer	GGGTACCCACGCGAATCAC	19		

HPRT1	Forward primer	TGACACTGGCAAAACAATGCA	21
	Reverse primer	GGTCCTTTTCACCAGCAAGCT	21
RPLP1	Forward primer	CCTGGAGGAGAAGAGAGA	23
	Reverse primer	TTGAGGACCTCTGTGTATTTGTCAA	25
UBC	Forward primer	ATTTGGGTCGCGGTTCTTG	19
	Reverse primer	TGCCTTGACATTCTCGATGGT	21
YWHAZ	Forward primer	ACTTTTGGTACATTGTGGCTTCAA	24
	Reverse primer	CCGCCAGGACAAACCAGTAT	20
CXCL10	Forward primer	ACTGTACGCTGTACCTGCATCA	22
	Reverse primer	TCAGACACCTCTTCTCACCCTTC	23
CD69	Forward primer	CCAAGTTCCTGTCCTGTGC	21
	Reverse primer	CCTCTGGTAGCCAACCCAGT	20
CD103	Forward primer	CGTCCTCAAGAGGTCATCTGCT	22
	Reverse primer	GCCTGAATTGAAGGGTGTGG	20
GZMB	Forward primer	GTGCGAATCTGACTTACGCCAT	22
	Reverse primer	CTGGGCCACCTTGTTACACAC	21
CASP3	Forward primer	TGGCGTGTCATAAAATACCAGTG	24
	Reverse primer	CTTGTCGGCATACTGTTTCAGC	22
CASP7	Forward primer	CGGGGCCCATCAATGACACA	20
	Reverse primer	CTGGGCTCCTCCACGAGTAA	20
BCL2	Forward primer	GTGTGGAGAGCGTCAACC	20
	Reverse primer	GCCGTACAGTTCCACAAAGGC	21
IFNG	Forward primer	GCATCCAAAAGAGTGTGGAGACC	23
	Reverse primer	TAGCTGCTGGCGACAGTTCA	23
TGFB	Forward primer	CGA GCC CTG GAC ACC AAC TAT T	22
	Reverse primer	GAA GTT GGC ATG GTA GCC CTT G	22

Supplementary Table S2. Correlations of genes with dimensions according to Factominer Dimdes function..

Dim1					
	correlation	P-value			
FOXP3	0.87	4.45E-24			
CD103	0.83	3.67E-20			
CD69	0.81	4.29E-18			
	R2	P-value			
Group	0.23	0.0012			
	Estimate	P-value			
Group=GII	1.27	8.48881E-05			
Group=IV	-0.74	0.026			
Dim2					
	correlation	P-value			
CD69	0.56	1.68261E-07			
CD103	-0.44	7.14151E-05			
	Estimate	P-value			
Group=GIII	0.343	0.047			

Supplementary Table S3. Wilconxon paired analysis. A- Treatment with Mambisa, B- Treatment with Abdala.

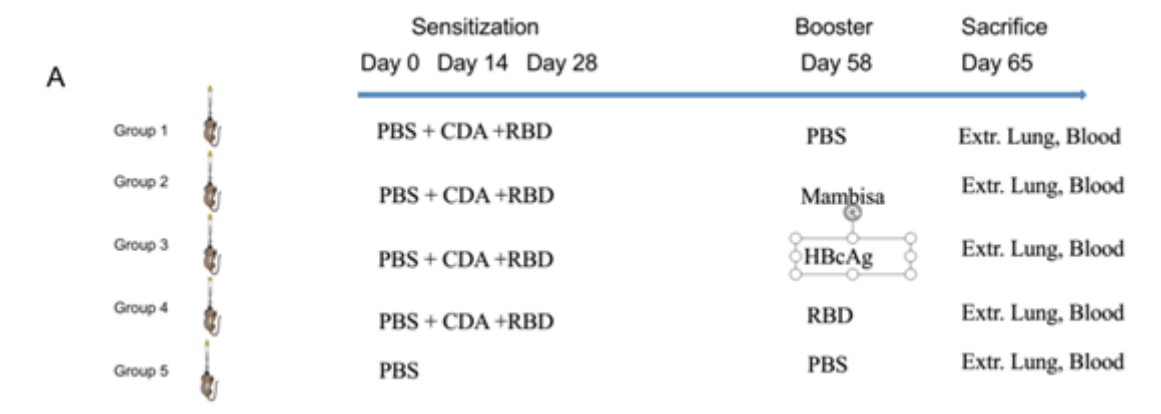
Δ

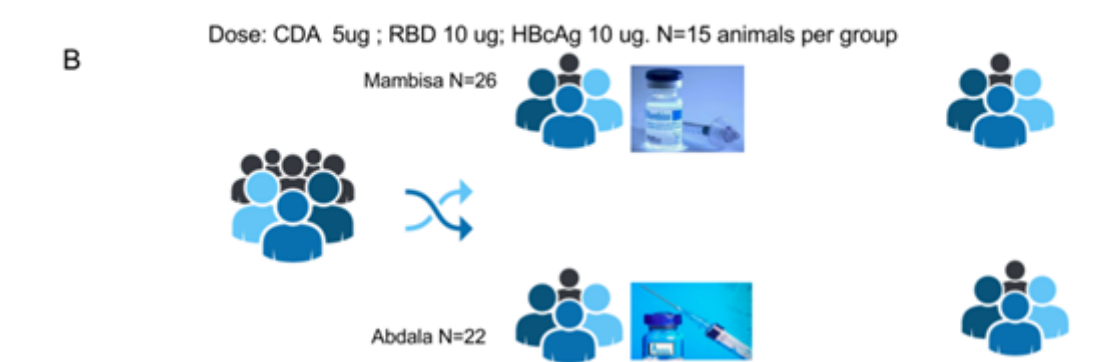
Group 1	Group 2	p-Value
INFG (T1 M)	INFG (T0 M)	1.424E-03
CD69 (T1 M)	CD69 (T0 M)	4.617E-03
GZMB (T1 M)	GZMB (T0 M)	2.456E-02
CXCL10 (T1 M)	CXCL10 (T0 M)	4.328E-02
CASP3 (T1 M)	CASP3 (T0 M)	5.861E-02
CD103 (T1 M)	CD103 (T0 M)	1.172E-01
BCL2 (T1 M)	BCL2 (T0 M)	4.903E-01
TGFB1 (T1 M)	TGFB1 (T0 M)	8.392E-01

В

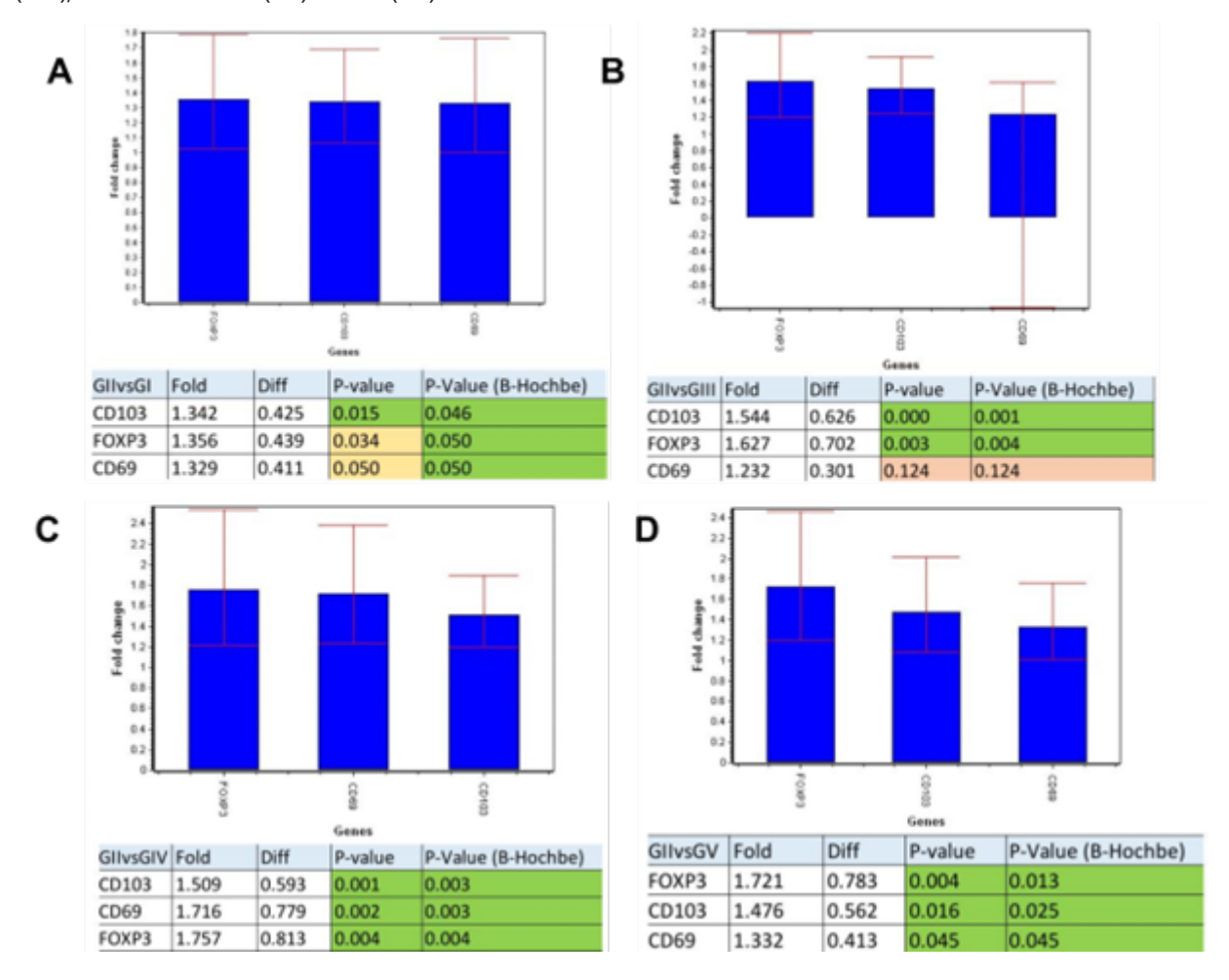
Group 1	Group 2	p-Value
INFG (T1 A)	INFG (T0 A)	1.14E-01
CASP3 (T1 A)	CASP3 (T0 A)	4.53E-01
CD103 (T1 A)	CD103 (T0 A)	5.07E-01
TGFB1 (T1 A)	TGFB1 (T0 A)	5.07E-01
CD69 (T1 A)	CD69 (T0 A)	6.55E-01
CXCL10 (T1 A)	CXCL10 (T0 A)	6.55E-01
GZMB (T1 A)	GZMB (T0 A)	6.55E-01
BCL2 (T1 A)	BCL2 (T0 A)	7.52E-01

Supplementary Figure S1. Inmunization scheme, A study in mouse, B study in humans.





Supplementary Figure S2. Result of mean comparisons between groups for each gene according to the t-test with p-value correction for multiple comparisons. A- Mambisa (GII) vs PBS/sensitized (GI), B- Mambisa (GII) vs HBcAg (GIII), C- Mambisa (GII) vs RBD (GIV), and D- Mambisa (GII) vs PBS (GV).



REFERENCES

- Mathieu E, Ritchie H, Rodés-Guirao L, Appel C, Giattino C, Hasell J, et al. Coronavirus Pandemic (COVID-19). Our World in Data [Internet]. 2020 Mar 5 [cited 2024 Mar 12]; Available from: https://ourworldindata.org/covid-vaccinations.
- Más-Bermejo PI, Dickinson-Meneses FO, Almenares-Rodríguez K, Sánchez-Valdés L, Guinovart-Díaz R, Vidal-Ledo M, et al. Correction to "Cuban Abdala vaccine: Effectiveness in preventing severe disease and death from COVID-19 in Havana, Cuba; A cohort study" [The Lancet Regional Health Americas 2022; 16: 100366] https://doi.org/10.1016/j.lana.2022.100366. Lancet Reg Health Am. 2023 Feb;18:100422.
- 3. Mambisa, one of the five nasal COVID-19 vaccine candidates in the world. 2024 Mar 12 [cited 2024 Mar 12]; Available from: https://www.bmj.com/content/373/bmj.n1346/rr-1.

- 4. Estudio MAMBISA | Registro Público Cubano de Ensayos Clínicos [Internet]. [cited 2024 Mar 12]. Available from: https://rpcec.sld.cu/ensayos/RPCEC00000345-Sp.
- 5. Orumaa K, Dunne MR. The role of unconventional T cells in COVID-19. Ir J Med Sci. 2022 Apr 1;191(2):519–28.
- Limonta-Fernández M, Chinea-Santiago G, Martín-Dunn AM, Gonzalez-Roche D, Bequet-Romero M, Marquez-Perera G, et al. An engineered SARS-CoV-2 receptorbinding domain produced in Pichia pastoris as a candidate vaccine antigen. New Biotechnology. 2022 Dec 25;72:11–21.
- 7. Lemos-Perez G, Chavez-Valdes S, Gonzalez-Formental H, Freyre-Corrales G, Vazquez-Arteaga A, Alvarez-Acevedo B, et al. Elevated Antibody Titers in Abdala Vaccinees Evaluated by Elecsys® Anti-SARS-Cov-2 S Highly Correlate with UMELISA SARS-Cov-2 ANTI RBD, ACE-2 Binding Inhibition and Viral Neutralization Assays. J Biotechnol Biomed [Internet]. 2022 [cited 2025 Feb 21];05(03). Available from: https://www.fortunejournals.

- com/articles/elevated-antibody-titers-in-abdala-vaccinees-evaluated-by-elecsysreg-antisarscov2-shighly-correlate-with-umelisa-sarscov2-anti-rb.html.
- Ebensen T, Yevsa T, Morr M, Guzmán C. Bis-(3',5')-cyclic dimeric adenosine monophosphate: strong Th1/Th2/Th17 promoting mucosal adjuvant. Vaccine [Internet]. 2011 Jul 18 [cited 2025 Feb 21];29(32). Available from: https://pubmed.ncbi.nlm.nih.gov/21619907/
- Bergkvist A, Rusnakova V, Sindelka R, Garda JMA, Sjögreen
 Lindh D, et al. Gene expression profiling Clusters of possibilities. Methods. 2010 Apr 1;50(4):323–35.
- 10. Andersen CL, Jensen JL, Ørntoft TF. Normalization of real-time quantitative reverse transcription-PCR data: a model-based variance estimation approach to identify genes suited for normalization, applied to bladder and colon cancer data sets. Cancer Res. 2004 Aug 1;64(15):5245–50.
- Vandesompele J, De Preter K, Pattyn F, Poppe B, Van Roy N, De Paepe A, et al. Accurate normalization of real-time quantitative RT-PCR data by geometric averaging of multiple internal control genes. Genome Biology. 2002 Jun 18;3(7):research0034.1.
- Xie F, Xiao P, Chen D, Xu L, Zhang B. miRDeepFinder: a miRNA analysis tool for deep sequencing of plant small RNAs. Plant Mol Biol. 2012 Jan 31;
- 13. Pfaffl MW, Tichopad A, Prgomet C, Neuvians TP. Determination of stable housekeeping genes, differentially regulated target genes and sample integrity: BestKeeper--Excel-based tool using pair-wise correlations. Biotechnol Lett. 2004 Mar;26(6):509–15.
- 14. Silver N, Best S, Jiang J, Thein SL. Selection of housekeeping genes for gene expression studies in human reticulocytes using real-time PCR. BMC Molecular Biology. 2006 Oct 6;7(1):33.
- 15. Giuliani A. The application of principal component analysis to drug discovery and biomedical data. Drug Discov Today. 2017 Jul;22(7):1069–76.
- Cozzolino D, Power A, Chapman J. Interpreting and Reporting Principal Component Analysis in Food Science Analysis and Beyond. Food Anal Methods. 2019 Nov;12(11):2469–73.
- 17. Chapman S, Schenk P, Kazan K, Manners J. Using

- biplots to interpret gene expression patterns in plants. Bioinformatics. 2002 Jan;18(1):202–4.
- 18. Gabriel KR. The Biplot Graphic Display of Matrices with Application to Principal Component Analysis on JSTOR. Biometrika. 1971 Dec;58(3):433–367.
- 19. Szabo PA, Miron M, Farber DL. Location, location, location: Tissue resident memory T cells in mice and humans. Sci Immunol. 2019 Apr 5;4(34):eaas9673.
- Kumar BV, Kratchmarov R, Miron M, Carpenter DJ, Senda T, Lerner H, et al. Functional heterogeneity of human tissue-resident memory T cells based on dye efflux capacities. JCI Insight. 2018 Nov 15;3(22):e123568.
- 21. Uddback IEM, Mattingly C, Thomas J, Kost KN, Li ZRT, Thomsen AR, et al. Resident Memory CD8+ T cells in the respiratory tract prevent transmission of respiratory viruses. The Journal of Immunology. 2021 May 1;206(1_Supplement):103.01-103.01.
- 22. Molodtsov A, Turk MJ. Tissue Resident CD8 Memory T Cell Responses in Cancer and Autoimmunity. Front Immunol. 2018 Nov 29;9:2810.
- 23. Wang Q, Yang C, Yin L, Sun J, Wang W, Li H, et al. Intranasal booster using an Omicron vaccine confers broad mucosal and systemic immunity against SARS-CoV-2 variants. Sig Transduct Target Ther. 2023 Apr 17;8(1):1–9.
- 24. Takamura S. Niches for the Long-Term Maintenance of Tissue-Resident Memory T Cells. Front Immunol. 2018;9:1214.
- Primorac D, Vrdoljak K, Brlek P, Pavelić E, Molnar V, Matišić V, et al. Adaptive Immune Responses and Immunity to SARS-CoV-2. Front Immunol. 2022 May 4;13:848582.
- 26. Tun ZH, Htike NTT, Kyi-Tha-Thu C, Lee WH. Employing T-Cell Memory to Effectively Target SARS-CoV-2. Pathogens. 2023 Feb 11;12(2):301.
- 27. Goliwas KF, Wood AM, Simmons CS, Khan R, Khan SA, Wang Y, et al. Local SARS-CoV-2 Peptide-Specific Immune Responses in Lungs of Convalescent and Uninfected Human Subjects [Internet]. Infectious Diseases (except HIV/AIDS); 2021 [cited 2024 Nov 15]. Available from: http://medrxiv.org/lookup/doi/10.1101/2021.09.02.212 63042.

- 28. Niessl J, Sekine T, Buggert M. T cell immunity to SARS-CoV-2. Seminars in Immunology. 2021 Jun;55:101505.
- 29. Schoenborn JR, Wilson CB. Regulation of interferongamma during innate and adaptive immune responses. Adv Immunol. 2007;96:41–101.
- 30. Qin XJ, Lin X, Xue G, Fan HL, Wang HY, Wu JF, et al. CXCL10 is a potential biomarker and associated with immune infiltration in human papillary thyroid cancer. Biosci Rep. 2021 Jan 7;41(1):BSR20203459.
- 31. Reassessing granzyme B: unveiling perforinindependent versatility in immune responses and therapeutic potentials PubMed [Internet]. [cited 2025 Mar 6]. Available from: https://pubmed.ncbi.nlm.nih.gov/38846935/
- 32. Nateghi-Rostami M, Sohrabi Y. Memory T cells: promising biomarkers for evaluating protection and vaccine efficacy against leishmaniasis. Front Immunol. 2024 Feb 26;15:1304696.
- 33. Bending D, Paduraru A, Ducker CB, Prieto Martín P, Crompton T, Ono M. A temporally dynamic Foxp3 autoregulatory transcriptional circuit controls the effector Treg programme. EMBO J. 2018 Aug 15;37(16):e99013.
- 34. Mercer F, Unutmaz D. The biology of FoxP3: a key player in immune suppression during infections, autoimmune diseases and cancer. Adv Exp Med Biol. 2009;665:47–59.
- 35. Ferreira C, Barros L, Baptista M, Blankenhaus B, Barros A, Figueiredo-Campos P, et al. Type 1 Treg cells promote the generation of CD8+ tissue-resident memory T cells. Nat Immunol. 2020 Jul;21(7):766–76.
- 36. Graham JB, Da Costa A, Lund JM. Regulatory T cells shape the resident memory T cell response to virus infection in the tissues. J Immunol. 2014 Jan 15;192(2):683–90.
- 37. de Goër de Herve MG, Jaafoura S, Vallée M, Taoufik Y. FoxP3+ regulatory CD4 T cells control the generation of functional CD8 memory. Nat Commun. 2012;3:986.
- 38. Thanh TT, Tu NTK, Nguyet LA, Thuy CT, Thuan NLT, Ny NTH, et al. Immunogenicity of Abdala COVID-19 vaccine in Vietnamese people after primary and booster vaccinations: A prospective observational study in Vietnam. International Journal of Infectious Diseases. 2024 Oct 1;147:107173.

- 39. Más-Bermejo PI, Dickinson-Meneses FO, Almenares-Rodríguez K, Sánchez-Valdés L, Guinovart-Díaz R, Vidal-Ledo M, et al. Cuban Abdala vaccine: Effectiveness in preventing severe disease and death from COVID-19 in Havana, Cuba; A cohort study. Lancet Reg Health Am. 2022 Dec;16:100366.
- 40. Aguilar JC, Lobaina Y, Muzio V, García D, Pentón E, Iglesias E, et al. Development of a nasal vaccine for chronic hepatitis B infection that uses the ability of hepatitis B core antigen to stimulate a strong Th1 response against hepatitis B surface antigen. Immunol Cell Biol. 2004 Oct;82(5):539–46.
- 41. Pumpens P, Grens E. Hepatitis B core particles as a universal display model: a structure-function basis for development. FEBS Lett. 1999 Jan 8;442(1):1–6.
- 42. Fedatto PF, Sérgio CA, Paula MO e, Gembre AF, Franco LH, Wowk PF, et al. Protection conferred by heterologous vaccination against tuberculosis is dependent on the ratio of CD4(+) /CD4(+) Foxp3(+) cells. Immunology. 2012 Nov;137(3):239–48.